

Effect of Ar/O₂ gas ratios on the structure, electrical and optical properties of Na-doped ZnCdO film synthesized by magnetron sputtering

Zhong Hua¹ · Yanping Song¹ · Yingrui Sui¹ · Yanjie Wu¹ · Shiquan Lv¹ · Bin Yao² · Li Xiao¹ · Zhanwu Wang¹ · Xiaoyan Liu¹

Received: 16 January 2016 / Accepted: 25 April 2016 / Published online: 3 May 2016
© Springer Science+Business Media New York 2016

Abstract Na-doped ZnCdO films [ZCO:Na] were grown on quartz substrates at different ratios of argon to oxygen gas flow (Ar:O₂) by the radio frequency magnetron sputtering method. The influence of Ar:O₂ ratio on structure, electrical and optical properties was investigated by using X-ray diffraction, X-ray photoelectron spectroscopy, Transmission electron microscopy, Hall measurements (Hall), optical absorption spectra and Photoluminescence. Results indicated that all obtained ZCO:Na thin films possess the hexagonal wurtzite structure and free from the formation of secondary phases. As the Ar:O₂ ratios change from 1:5 to 5:1, at first the E_g increases with the Ar:O₂ ratios increasing and reaches a maximum value at the Ar:O₂ ratio of 1:1, then decreases evidently with the Ar:O₂ ratios increasing continually. It is found that the lower Ar:O₂ ratio is propitious to obtain n-type ZCO:Na film, while the relative higher Ar:O₂ ratio is required to obtain p-type ZCO:Na thin films. When the Ar:O₂ ratio is 1:1, the ZCO:Na film shows the best p-type conduction characteristics, which has a hole concentration of $1.13 \times 10^{16} \text{ cm}^{-3}$, Hall mobility of $2.54 \text{ cm}^2 \text{ V}^{-1} \text{ s}^{-1}$ and resistivity of $2.53 \times 10^2 \text{ } \Omega \text{ cm}$. In addition, the mechanism of the influence of Ar:O₂ ratio on the electrical and optical properties of the film as well as the mechanism of p-type conductivity was discussed in this work.

1 Introduction

In recent years, various materials for the applications of blue and ultraviolet (UV) light-emitting diodes (LEDs) and laser diodes (LDs) have been attracted much attention [1]. In these materials, ZnO has been regarded as one of the most promising candidates owing to the wide band gap (3.37 eV) and relatively large free exciton binding energy (60 meV) at room temperature [2, 3]. In order to achieve the potential application of ZnO, high quality of both n-type and p-type ZnO films are indispensable. Now, n-type ZnO films can be obtained easily, however, the realization of stable and reproducible p-type ZnO is difficult due to the asymmetric doping limitations, which impedes the application and development of ZnO optoelectronic device seriously [4]. Another important issue for developing ZnO-based optoelectronic device technology is the fabrication of ZnO-related alloys, which would enable the modulation of the band gap, thus accelerate the fabrications of the barrier layers and the quantum wells used in the hetero-junction device application. It is well known that alloy ZnO with CdO can tune the band gap from 3.37 to 2.3 eV depending upon the Cd concentration [5, 6], the luminescence of ZnCdO (ZCO) alloy compounds can cover the green, blue to UV light spectra. Therefore, ZCO is a suitable well layer material for ZnO/ZCO superlattices and quantum wells, which are the key elements in ZnO-based LED and LD devices [7, 8]. In order to exploit these ZnO/ZCO heterostructures in optoelectronic devices, one of the critical issues is to achieve stable and reproducible p-type ZCO. However, reports on the p-type ZCO are currently very limited.

According to the theory research, the valence-band maximum (VBM) position of CdO is higher than that of ZnO [9]. Thus, alloying ZnO with CdO will narrow the

✉ Yingrui Sui
syr.8@163.com

¹ Key Laboratory of Functional Materials Physics and Chemistry of the Ministry of Education, Jilin Normal University, Siping 136000, Jilin, China

² State Key Laboratory of Superhard Materials and College of Physics, Jilin University, Changchun 130023, Jilin, China

band gap and shift the valence-band edge to higher energy, thus decreasing the activation energy of the defect acceptor states, which exhibits advantages to obtain p-type behavior [10]. In addition, the replacement of the proper amount of Zn by Cd is not expected to induce a significant change in crystal structure and lattice constant due to the similarity of the ionic radii [11]. Furthermore, the role of Cd in ZCO alloy does not act as donor, which could not compensate for the acceptor doping. Therefore, choosing an appropriate acceptor and doping method is proven to be very important in the preparation of p-type ZCO. Recently considerable attentions are paid to the group-I doping for realizing p-type ZnO [12–14]. Na has been considered as one of the suitable choices for realizing p-type ZnO. p–n homojunction LEDs based on Na-doped p-type ZnO have been demonstrated [15, 16] and the room temperature electroluminescence has been observed by incorporating ZnMgO/ZnO multiple quantum wells into the LED structure [17].

Among various techniques, magnetron sputtering has been widely used to study ZnO films owing to its simplicity, low cost, low processing temperature and gives deposits of better adhesion and higher density than other methods. And, the magnetron sputtering is a widely used and versatile technique that allows us to monitor the growth by controlling relevant parameters like sputtering power and sputtering time, substrate temperature, sputtering gas, sputtering target, etc. On the sputtering efficiency and practical application side, radio frequency (RF) magnetron sputtering have an relative advantage over direct current (DC) magnetron sputtering. In the plus-minus period of RF voltage, electrons and positive ions can reach the target surface, respectively. Therefore, it can't accumulate positive charge and exclude ions in the surface of target. Moreover, the degree of ionization of the working gas can get up to 5–6 % in the RF magnetron sputtering. As a result, RF magnetron sputtering can be used to fabricate all kinds of thin film materials, including metals, semiconductors, insulators, alloys, compounds, etc. In this work, ZCO:Na films were grown by RF magnetron sputtering in the Ar + O₂ ambient with different ratios of argon to oxygen gas flow (Ar:O₂). The effect of Ar:O₂ ratio on the structure, optical, electrical properties of ZCO:Na films was investigated in detail. The p-type ZCO:Na films were obtained by changing the Ar:O₂ ratio and a possible formation mechanism of the p-type film is proposed.

2 Experimental procedures

A series of ZCO:Na thin films were prepared on quartz substrates by RF reactive magnetron sputtering technique. A compact ceramic target with a nominal component of Zn_{0.78}Cd_{0.2}Na_{0.02}O was used as sputtering target. The

quartz substrates were cleaned in an ultrasonic bath with acetone, ethanol and de-ionized water for 15 min sequentially at room temperature, and then washed using de-ionized water. For the growth of all films, the growth chamber was evacuated to a fundamental pressure of 2×10^{-4} Pa by a combination of mechanical pump and molecular pump, and then the mixed gases of Ar + O₂ were introduced as the working gas with a constant total pressure about 1 Pa. Argon and oxygen of 99.99 % purity were introduced through separate mass flow controllers. Total mass flow was 60 sccm and the Ar:O₂ ratio was controlled at 1:5, 1:2, 1:1, 2:1 and 5:1, respectively. The sputtering power was 100 W. Prior to deposition, pre-sputtering for 10 min to remove the surface oxide formed during air exposure. The substrates were held at 500 °C during the film deposition and the deposition time of 60 min was maintained for all samples. Finally, the as-sputtered films were annealed in atmosphere for 30 min at a temperature of 620 °C. In order to avoid surface contamination, the films were placed in a quartz boat, which was put into a quartz tube. This quartz tube was then inserted into the furnace.

Crystal structure of the samples were characterized by X-ray diffraction (JapanRigaku D/max-ga X-ray diffractometer) using CuK α ($\lambda = 0.15406$ nm) and Transmission electron microscope (TEM-2100). Compositions and chemical state of elements in the ZCO:Na thin films were detected by X-ray photoelectron spectroscopy (XPS) (ESCALAB MARK II, VG Inc.) using an Al K α as X-ray source. The electrical properties were carried out with Van der Pauw configuration in a Hall-effect measurement system. The room-temperature absorbance measurement was performed using an UV–Vis–near-infrared (NIR) spectrophotometer (UV-3101PC). Photoluminescence (PL) measurement was performed at room temperature by the excitation from a 325 nm He–Cd laser.

3 Results and discussion

Figure 1 shows the XRD diffraction patterns of ZCO:Na thin films fabricated at different Ar:O₂ ratios: (a) 1:5, (b) 1:2, (c) 1:1, (d) 2:1 and (e) 5:1, respectively. As shown in Fig. 1, a series of diffraction peaks are observed, which are attributed to the diffraction of (100), (002), (101) and (110) planes of ZnO (ICDD card #36-1451) with hexagonal wurtzite structure, respectively. It is a typical indication that the films are polycrystalline in nature. Also, apart from ZnO characteristic peaks, no other peak corresponding to either cadmium, zinc and sodium or their complex oxide were detected from the ZCO:Na sample, which reveals clearly that doped Cd and Na does not change the basic structure of ZnO and existed in the form of impurity atoms,

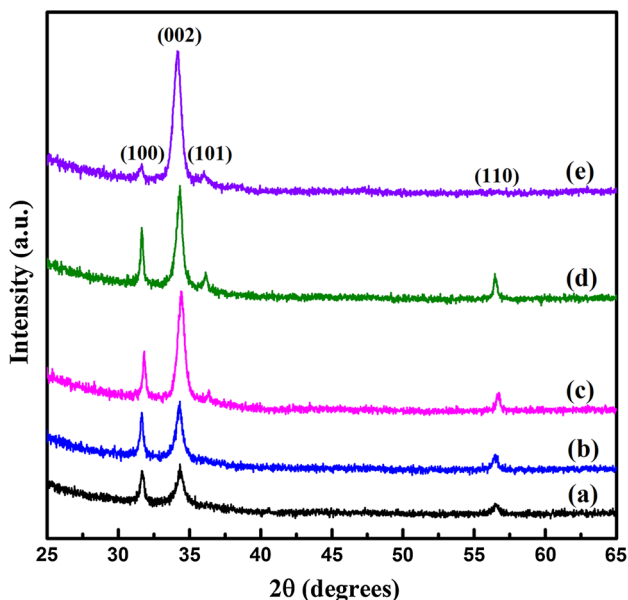


Fig. 1 (Color online) X-ray diffraction patterns of ZCO:Na thin films deposited at different Ar:O₂ ratios: *a* 1:5, *b* 1:2, *c* 1:1, *d* 2:1 and *e* 5:1, respectively

that is, the Cd²⁺ ions and Na⁺ ions would uniformly substitute into the Zn²⁺ sites or interstitial sites in ZnO lattice. It can be seen from Fig. 1 that as the Ar:O₂ ratio increases from 1:5 to 5:1, the (101) peak appears at higher Ar:O₂ ratio, but the intensity is very weak, meanwhile the (100) peak is getting diminished as Ar:O₂ ratio approaches 5:1. It also can be found that the relative intensity of (002) diffraction peak changes apparently, the peak intensity of samples prepared at higher Ar:O₂ ratio are obviously stronger than that of samples prepared at lower Ar:O₂ ratio, which could be observed clearly in Table 1 (in later). It is well known that the crystal plane of (100) and (002) is vertical, the crystal plane of (101) and (002) is oblique crossing, therefore, it is concluded that ZCO:Na thin films are easier to grow along the (002) orientation at higher Ar:O₂ ratio.

The peak position 2θ, full-width at half-maximum (FWHM) and the peak intensity are obtained from (002) diffraction peak in the XRD profile and summarized in

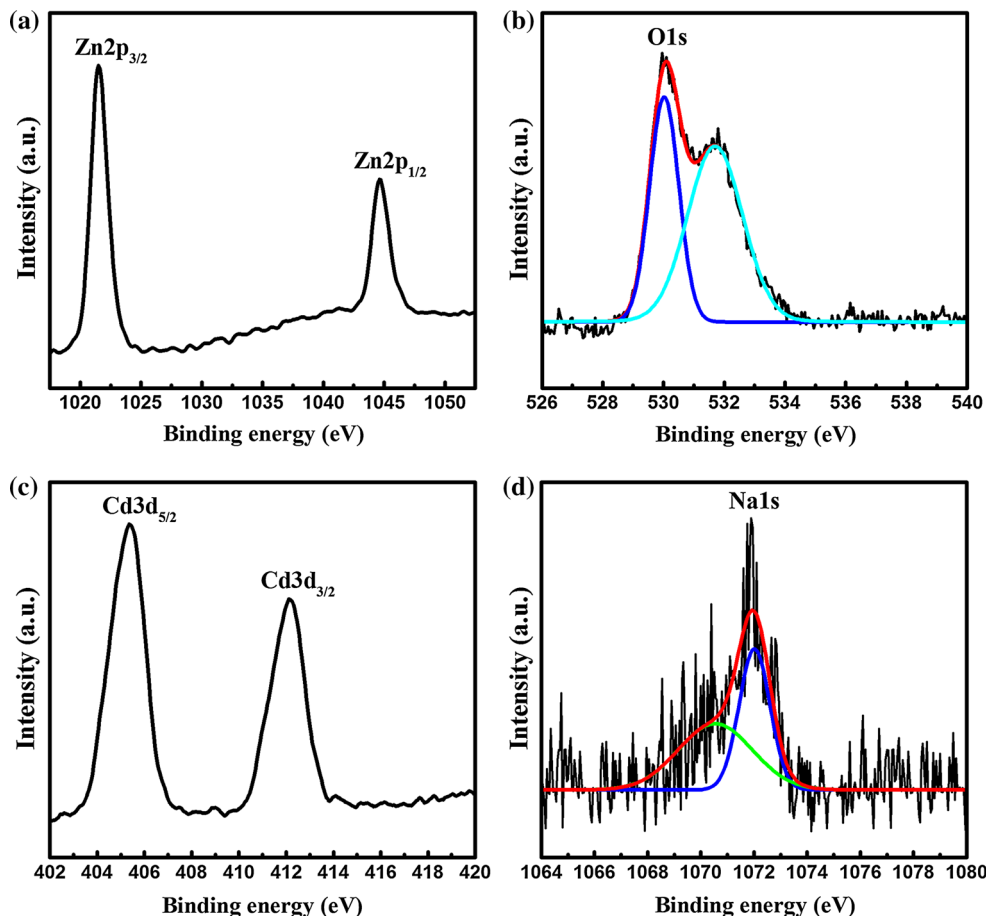
Table 1 Summary of the 2θ, FWHM, intensity of (002) peak for ZCO:Na films fabricated at different Ar:O₂

Samples (Ar:O ₂)	2θ (deg)	FWHM (deg)	Intensity (a.u.)
1:5	34.343	0.632	118
1:2	34.260	0.618	170
1:1	34.396	0.616	370
2:1	34.296	0.537	335
5:1	34.144	0.647	478

Table 1. It is observed that the (002) diffraction peaks of all films shift toward the lower diffraction angle side compared with that of standard ZnO (34.42°) (ICDD card #36-1451). It is an indication of increment in the lattice parameter *c* of all films, which is probably attributed to the fact that Cd and Na have been doped into ZnO, and the substitution of larger Cd (with ionic radius 0.97 Å) and larger Na (with ionic radius 1.02 Å) for the sites of smaller Zn (with ionic radius 0.74 Å) in the ZnO crystal lattice took place. It can be seen that the FWHM value floats up and down slightly (from 0.537° to 0.647°) as the Ar:O₂ ratio increases up from 1:5 to 5:1. However, (002) diffraction peak relative intensity changes apparently, the peak intensity of samples prepared at the Ar:O₂ ratio of 1:1, 2:1 and 5:1 are obviously stronger than that of samples prepared at the Ar:O₂ ratio of 1:5 and 1:2, indicating that the higher oxygen content in deposition process may induces defects in thin films, which lead to the degradation of crystalline quality by inhibiting the grain growth by excess oxygen segregation at the grain boundaries [18]. It is concluded that the ZCO:Na films prepared at higher Ar:O₂ ratio process better crystal quality.

XPS is a sensitive and powerful method of yielding comprehensive information about elemental content and chemical bonding states. In order to identify phase compositions and chemical state of elements of Zn, O, Cd and Na in the ZCO:Na films, XPS measurements were performed for ZCO:Na film deposited at the Ar:O₂ ratio of 5:1. Prior to XPS measurements, the sample was cleaned by Ar⁺ ion bombardment for 120 s to remove any potential surface contamination. Figure 2a–d display the XPS spectra of the core level regions of Zn2*p*, O1*s*, Cd3*d* and Na1*s* for the ZCO:Na film deposited at the Ar:O₂ ratio of 5:1. The Zn2*p* XPS spectrum is illustrated in Fig. 2a, it can be observed that the peaks located at 1021.5 and 1044.6 eV were associated to the Zn2*p*_{3/2} and Zn2*p*_{1/2}, respectively. The binding energy of the Zn2*p* is almost the same with that of Zn²⁺ in ZnO crystal, which is ascribed to the binding energy of the zinc atom that exists in Zn–O [19]. What’s more, according to the opinion of Sáaedi et al. [20], the spin–orbit splitting of 23.1 eV for Zn2*p*_{3/2} and Zn2*p*_{1/2} confirm that the Zn atoms are in a completely oxide state. Figure 2b presents the O1*s* XPS spectrum of the ZCO:Na film deposited at the Ar:O₂ ratio of 5:1, which can be deconvoluted into two strong peaks, indicating the existence of two different oxygen environments [21, 22]. One peak with a lower binding energy of 530.02 eV originated from the O–Zn bond formation, which is attributed to O^{2–} on the wurtzite structure of the hexagonal Zn²⁺ ion array, surrounded by Zn atoms with their full complement of nearest neighbor O^{2–} [23]. The higher binding energy peak at 531.69 eV derives from the surface adsorbed oxygen,

Fig. 2 (Color online) XPS spectra of **a** Zn2p, **b** O1s, **c** Cd3d and **d** Na1s for ZCO:Na thin films deposited at the Ar:O₂ ratio of 5:1



which is possibly attributed to environmental moisture trapped on the film surface.

As shown in Fig. 2c, two strong peaks appeared at 404.45 and 412.15 eV, which are attributed to the binding energy of Cd3d_{5/2} and Cd3d_{3/2}, respectively. The binding energy of the Cd3d is almost the same with that of Cd²⁺ in ZCO alloy films [24], which are attributed to the binding energy of the cadmium atom that exists in Cd–O. No evidence of the metallic Cd peak or other valance state was observed, which confirmed that Cd exist only in the oxidized state. These results indicate that Cd has been doped into ZnO and occupied the sites of Zn atoms in the ZnO crystal lattice to form the ZCO:Na film, which is in agreement with the results of XRD analysis. Figure 2d illustrates Na1s core level spectrum of ZCO:Na film deposited at the Ar:O₂ ratio of 5:1. The spectrum was deconvoluted into two peaks using Gaussian fitting method and the deconvolution revealed the presence of two different Na1s peaks in the film. One peak with a higher binding energy of 1071.89 eV is assigned to arise from Na–O bond [25], which indicates that the Na atom substitutes for the Zn atom to form the Na_{Zn} acceptor in ZCO:Na film. Another peak with a lower binding energy of

1070.45 eV is usually attributed to the presence of a Na₂C₂O₄ phase in the sample [26]. The Na₂C₂O₄ phase could be formed by absorbing carbon originating from the contamination from oil-diffusion pump. It was found from Fig. 2d that the intensity of 1071.89 eV peak is much stronger than that of 1070.45 eV peak, indicating that a great amount of Na elements exist in the form of Na_{Zn} acceptor, yet a very small amount of Na elements exist in the form of Na₂C₂O₄ in the ZCO:Na film.

According to the rules of quantitative analysis of the XPS spectrum, the relative atomic surface concentrations can be determined using the integrated area of Zn2p, O1s, Cd3d and Na1s peaks, the Zn, O, Cd and Na content can be evaluated approximately 30.1, 63.6, 5.9 and 0.4 at.% in the ZCO:Na film prepared at the Ar:O₂ ratio of 5:1, respectively. It has been found that the concentration of O is greater than that of Zn. The large difference between zinc and oxygen content also supports the fact that Cd and Na substitute for the Zn atom sites (Cd_{Zn} and Na_{Zn}) in the ZCO:Na film. The Cd content with 5.9 at.% was significantly larger than the thermodynamic solid solubility limits (2 at.%). Moreover, the Cd content in the film was lower than that in the corresponding target, which can be mainly

attributed to the limiting sputtering efficiency and the fact that zinc is more lively than cadmium. It also can be found that the Na has been doped into the film and provided a lower composition of Na compared to the corresponding target, which is probably due to the large size difference between Zn and Na, and thus limits the solubility of Na in ZnO lattice [27].

In order to better reveal the detailed microscopic structure of the films, an ZCO film was grown on an quartz substrate under the same experimental conditions as ZCO:Na film prepared at the Ar:O₂ ratio of 5:1. High-resolution transmission electron microscope (HRTEM) measurements were performed for the ZCO and ZCO:Na films prepared at the Ar:O₂ ratio of 5:1, as shown in Fig. 3. Figure 3a shows the HRTEM lattice image of ZCO grains, a lattice spacing of 0.2617 nm was observed,

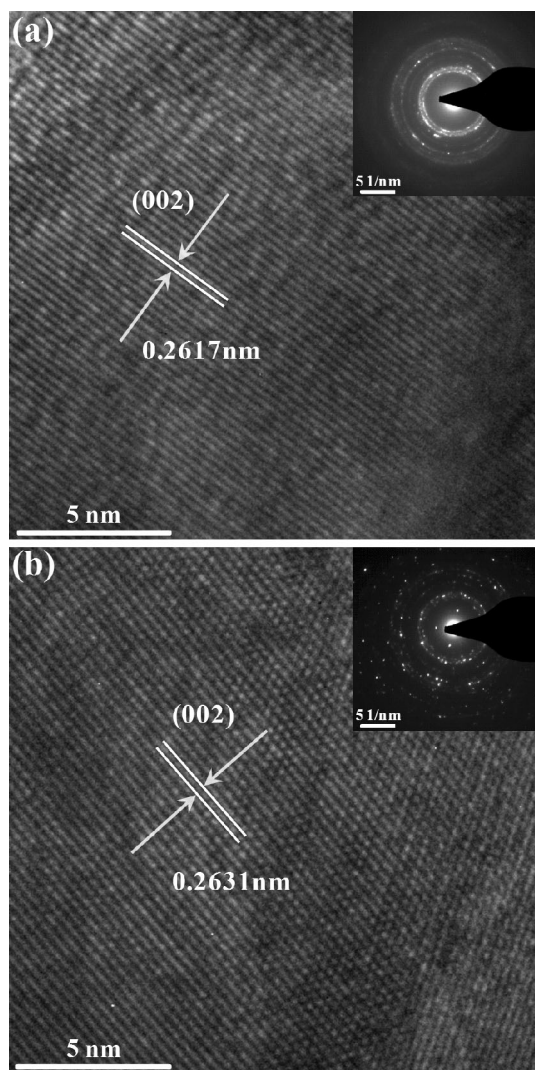


Fig. 3 High resolution TEM of **a** ZCO and **b** ZCO:Na thin films deposited at the Ar:O₂ ratio of 5:1. Scar bar 5 nm. Top inset SAED pattern corresponding to the film

corresponding to the spacing of the (002) plane of wurtzite ZnO (ICDD card #80-0074). However, this spacing is bigger than that (0.2603 nm) of standard ZnO, since Cd²⁺ ion has a radius of 0.97 Å, which is larger than that (0.74 Å) of Zn²⁺ ion, suggesting that Cd atoms substitute for the Zn atom sites in the ZnO crystal lattice to form the ZCO film. Figure 3b displays the HRTEM lattice image of ZCO:Na grains which is aligned in the [002] direction, the lattice spacing measured from the lattice image is 0.2631 nm. It can be observed that the measured lattice spacing (0.2631 nm) of the (002) crystallographic plane of ZCO:Na grain is larger than that (0.2617 nm) of ZCO grain. Since the ionic radius of Na (1.02 Å) is larger than that of Zn (0.74 Å) and Cd (0.97 Å), therefore, it is concluded that Na and Cd atoms simultaneously substitute for the Zn atom sites in the ZnO crystal lattice to form the ZCO:Na film, which is in agreement with the results of XRD analysis. The selected-area electron diffraction (SAED) patterns show typical polycrystalline diffraction for two samples, indicating that the two samples belong to highly crystalline material, as shown in upper right inset.

The electrical properties and the nature (p-type or n-type) of conduction in the samples were investigated by Vander Pauw Hall measurements at room temperature. Table 2 summarizes the electrical properties of the ZCO:Na thin films prepared at different Ar:O₂ ratio. To examine the reliability and repeatability of the conduction of the films, the electrical measurements were performed several times, and much the same results were obtained as expected. It has been observed that the ZCO:Na film prepared at the Ar:O₂ ratio of 1:5 exhibits vague conduction type, which is probably attributed to the doping inhomogeneities self-compensation effect caused by intrinsic defects [28–30]. When the Ar:O₂ ratios change from 1:5 to 1:1, the conductivity of ZCO:Na films changed dramatically from vague type to n-type, finally changed to p-type. When the Ar:O₂ ratio is 1:1, the film shows the best p-type conduction characteristics with a hole concentration of $1.13 \times 10^{16} \text{ cm}^{-3}$, Hall mobility of $2.54 \text{ cm}^2 \text{ V}^{-1} \text{ s}^{-1}$ and resistivity of $2.53 \times 10^2 \text{ } \Omega \text{ cm}$. When the Ar:O₂ ratio continues to increase up to 5:1, the ZCO:Na film still displays p-type conduction characteristics, but the hole concentration is about one order magnitude lower than that of the ZCO:Na film prepared at the Ar:O₂ ratio of 1:1. It is found that lower Ar:O₂ ratio is propitious to obtain n-type ZCO:Na film, while relative higher Ar:O₂ ratio is required to obtain p-type ZCO:Na thin films. The p-type ZCO:Na films with better electrical properties can be obtained by adjusting the Ar:O₂ ratio during film deposition.

To study the effect of Ar:O₂ ratio on the optical band gap of ZCO:Na films, the absorption edges were investigated by an UV–Vis–NIR spectrophotometer. The theory of optical transition [31] can be used to express the relation

Table 2 Electrical properties of ZCO:Na films deposited at different Ar:O₂

Samples (Ar:O ₂)	Annealing temperature (°C)	Resistivity (Ω cm)	Carrier concentration (cm ⁻³)	Mobility (cm ² V ⁻¹ s ⁻¹)	Type
1:5	620	2.17E+2	4.77E+16	11.01	p/n
1:2	620	2.60E+2	3.35E+15	7.70	n
1:1	620	2.53E+2	1.13E+16	2.54	p
2:1	620	1.58E+2	5.55E+17	26.64	p/n
5:1	620	1.13E+2	3.23E+15	18.48	p

between absorption coefficient (α) and the photon energy ($h\nu$) for the direct transition as follows:

$$(\alpha h\nu)^{1/n} = A(h\nu - E_g) \quad (1)$$

where A is the band edge constant, E_g is the optical band gap and 'n' take the values 1/2, 3/2, 2 and 3, when the transitions are direct allowed, direct forbidden, indirect allowed and indirect forbidden, respectively. The ZnCdO is considered as more suitable for direct band gap energy material and hence $n = 1/2$ is employed for experimental data. The variations of $(\alpha h\nu)^2$ versus $h\nu$ for ZCO:Na thin films deposited at different Ar:O₂ ratios: (a) 1:5, (b) 1:2, (c) 1:1, (d) 2:1 and (e) 5:1 are shown in Fig. 4. When $(\alpha h\nu)^{1/n} = 0$, $E_g = h\nu$. The E_g can be determined by extrapolations of the linear portion of the curve to the $h\nu$ axis as $\alpha = 0$. The E_g variations with different Ar:O₂ ratios are given in the upper left inset. When the Ar:O₂ ratios change from 1:5 to 1:1, the E_g increases gradually and reaches a maximum value of 3.16 eV at the ratio of 1:1.

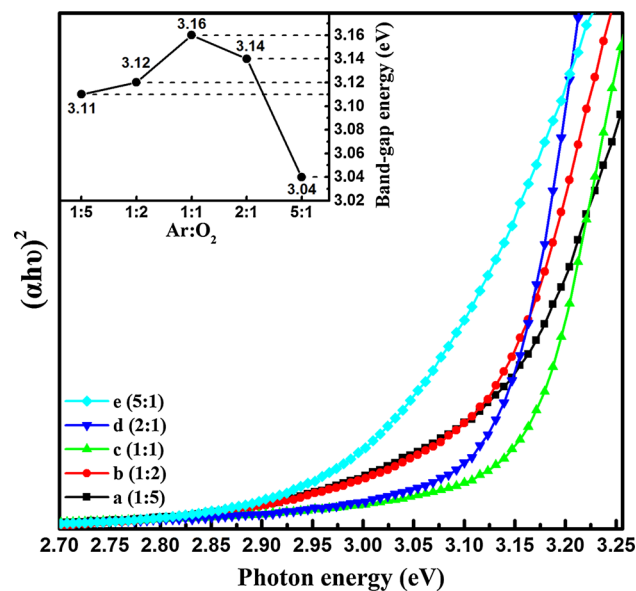


Fig. 4 (Color online) The curve of $(\alpha h\nu)^2$ versus $h\nu$ for ZCO:Na thin films deposited at different Ar:O₂ ratios: a 1:5, b 1:2, c 1:1, d 2:1 and e 5:1, respectively. The upper left inset shows the variation of E_g with different Ar:O₂ for ZCO:Na thin films

However, as the Ar:O₂ ratios continue to increase up to 5:1, the E_g decreases evidently to 3.04 eV. As we all know, in the magnetron sputtering process, high purity Ar were ionized into Ar⁺ and used as sputtering gas, therefore, the efficiency of bombard ceramic target with Ar⁺ could be influenced by the partial pressure of argon; On the other hand, high purity O₂ were ionized into O²⁻ and deposited on the substrate. In the present work, the total pressure of Ar and O₂ is constant, as the Ar partial pressure increases, which makes the O₂ partial pressure to reduce constantly, a part of Cd atoms cannot react with O atoms sufficiently and arrive the sites of crystal lattice. Therefore, in the beginning, the E_g increases with the Ar:O₂ ratios increasing and reaches a maximum value at the ratio of 1:1. As the Ar:O₂ ratios increases continually, the Ar partial pressure is increased and the sputtering yield is enhanced, therefore, Cd can react more easily with oxygen, more Cd atoms can reach crystal lattice and substitute for Zn atoms sites, so the E_g decreases accordingly.

To further investigate the optical properties of samples, the room PL measurements were performed for ZCO:Na thin films. Figure 5 shows PL spectra of ZCO:Na thin films deposited at different Ar:O₂ ratios: (a) 1:5, (b) 1:2, (c) 1:1, (d) 2:1 and (e) 5:1, respectively. It can be observed from Fig. 5 that there are two region obvious emission bands. One is defects related to visible light (VL) emission band in the range of 2.25–2.45 eV, which belongs to the yellow band (YB) relating to O_i. [32], the emissions at visible range usually are attributed to the existence of various defects related to zinc and oxygen [33]. The other one is in the region from 2.75 to 3.25 eV, the peak centered at approximately 3.15 eV in UV region, which are originate from a near-band-edge (NBE) transition of ZCO:Na thin films, namely the recombination of free excitons [34]. By comparison, an obvious interesting change was found from the PL spectra, the location of the emission peak in the UV region at first shift toward higher energy side with the increase of Ar:O₂ ratios from 1:5 to 1:1, then shift toward lower energy side with the increase of Ar:O₂ ratios from 1:1 to 5:1, which corresponding well with the variation trend of E_g deduced from absorption spectra in Fig. 4. The peak centered at about 2.77 eV is blue band (BB), which is

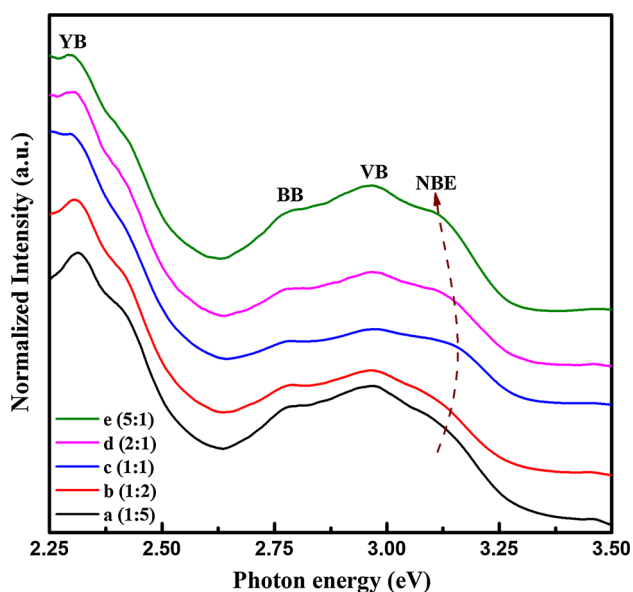


Fig. 5 (Color online) The room temperature PL spectra of ZCO:Na thin films deposited at different Ar:O₂ ratios: *a* 1:5, *b* 1:2, *c* 1:1, *d* 2:1 and *e* 5:1, respectively

attributed to the exciton recombination between the electron localized at the Zn_i and the holes in the valence [35]. The peak centered at approximately 2.96 eV is violet band (VB) emission, which originates from the defect emission of Zn vacancies (V_{Zn}) related to a shallow acceptor state. It has been reported that in nominally undoped ZnO, V_{Zn} is commonly considered as the dominant defect responding to the p-type conductivity, p-type conductivity of the undoped ZnO is due to contribution of V_{Zn} [36–39]. In combination with experimental results mentioned above, it is concluded that p-type conduction of ZCO:Na films comes from the contribution of V_{Zn} and Na_{Zn} acceptors.

4 Conclusions

In summary, a series of ZCO:Na films were grown on quartz substrates at different Ar:O₂ ratio by RF magnetron sputtering. The structure, optical and electrical properties of ZCO:Na films were found to be dependent on the Ar:O₂ ratio in the sputtering gas mixture. It is found that the ZCO:Na films prepared at higher Ar:O₂ ratio process better crystal quality. Meanwhile, the relative higher Ar:O₂ ratio is required to obtain p-type ZCO:Na thin films. As the Ar:O₂ ratios change from 1:5 to 5:1, at first the E_g increases and reaches a maximum value of 3.16 eV at the Ar:O₂ ratio of 1:1, then decreases evidently to 3.04 eV with the Ar:O₂ ratios increasing. By changing Ar:O₂ ratio, the ZCO:Na film with the best p-type conduction characteristics was obtained when Ar:O₂ ratio is 1:1. It has a hole concentration of

$1.13 \times 10^{16} \text{ cm}^{-3}$, Hall mobility of $2.54 \text{ cm}^2 \text{ V}^{-1} \text{ s}^{-1}$ and resistivity of $2.53 \times 10^2 \Omega \text{ cm}$. The p-type conductivity is mainly attributed to the contribution of Na_{Zn} and V_{Zn} acceptors.

Acknowledgments The authors would like to thank financial support of the National Natural Science Foundation of China under Grant Nos. 11254001, 61505067, 61475063, 11204104, the Program for the Development of Science and Technology of Jilin Province Grant No. 20150520086JH, the Program for New Century Excellent Talents in University Grant No. NCET-13-0824.

References

1. Y.S. Lee, S.N. Lee, I.K. Park, *Ceram. Int.* **39**, 3043 (2013)
2. O. Lupan, T. Pauporté, I.M. Tiginyanu, V.V. Ursaki, H. Heinrich, L. Chow, *Mater. Sci. Eng. B* **176**, 1277 (2011)
3. A. Aravinda, M.K. Jayaraj, M. Kumar, R. Chandra, *Mater. Sci. Eng. B* **177**, 1017 (2012)
4. Y.F. Yan, J.B. Li, S.H. Wei, M.M. Al-Jassim, *Phys. Rev. Lett.* **98**, 135506 (2007)
5. A. Janotti, C.G.V.D. Walle, *Rep. Prog. Phys.* **72**, 126501 (2009)
6. J.W. Mares, F.R. Ruhge, A.V. Thompson, P.G. Kik, A. Osinsky, B. Hertog, A.M. Dabiran, P.P. Chow, W.V. Schoenfeld, *Opt. Mater.* **30**, 346 (2007)
7. K. Yamamoto, T. Ohashi, T. Tawara, H. Gotoh, A. Nakamura, J. Temmyo, *Appl. Phys. Lett.* **93**, 171913 (2008)
8. K. Yamamoto, T. Tsuboi, T. Ohashi, T. Tawara, H. Gotoh, A. Nakamura, J. Temmyo, *J. Cryst. Growth* **312**, 1703 (2010)
9. Y.Z. Zhu, G.D. Chen, H.G. Ye, A. Walsh, C.Y. Moon, S.H. Wei, *Phys. Rev. B* **77**, 5209 (2008)
10. J.J. Chen, F. Ren, Y.J. Li, D.P. Norton, S.J. Peartona, A. Osinsky, J.W. Dong, P.P. Chow, J.F. Weaver, *Appl. Phys. Lett.* **87**, 2106 (2005)
11. D.W. Ma, Z.Z. Ye, H.M. Lu, J.Y. Huang, B.H. Zhao, L.P. Zhu, H.J. Zhang, P.M. He, *Thin Solid Films* **461**, 250 (2004)
12. W. Liu, F.X. Xiu, K. Sun, Y.H. Xie, K.L. Wang, Y. Wang, J. Zou, Z. Yang, J.L. Liu, *J. Am. Chem. Soc.* **132**, 2498 (2010)
13. L.D. Tang, B. Wang, Y. Zhang, Y.S. Gu, *Mater. Sci. Eng. B* **176**, 548 (2011)
14. M.K. Gupta, N. Sinha, B.K. Singh, B. Kumar, *Mater. Lett.* **64**, 1825 (2010)
15. S.S. Lin, J.G. Lu, Z.Z. Ye, H.P. He, X.Q. Gu, L.X. Chen, J.Y. Huang, B.H. Zhao, *Solid State Commun.* **148**, 25 (2008)
16. S.S. Lin, Z.Z. Ye, J.G. Lu, H.P. He, L.X. Chen, X.Q. Gu, J.Y. Huang, L.P. Zhu, B.H. Zhao, *J. Phys. D Appl. Phys.* **41**, 155114 (2008)
17. Z.Z. Ye, S.S. Lin, H.P. He, X.Q. Gu, L.X. Chen, J.G. Lu, J.Y. Huang, L.P. Zhu, L. Wang, Y.Z. Zhang, X.H. Li, *Chin. J. Semicond.* **29**, 1433 (2008)
18. S.S. Kim, B.T. Lee, *Thin Solid Films* **446**, 307 (2004)
19. S.N. Das, J.H. Choi, J.P. Kar, T.I. Lee, J.M. Myoung, *Mater. Chem. Phys.* **121**, 472 (2010)
20. A. Saaedi, R. Yousefi, F. Jamali-Sheini, M. Cheraghizade, A.K. Zak, N.M. Huang, *Ceram. Int.* **40**, 4327 (2014)
21. M.N. Islam, T.B. Ghosh, K.L. Chopra, H.N. Acharya, *Thin Solid Films* **280**, 20 (1996)
22. M. Chen, X. Wang, Y.H. Yu, Z.L. Pei, X.D. Bai, C. Sun, R.F. Huang, L.S. Wen, *Appl. Surf. Sci.* **158**, 134 (2000)
23. B.Q. Yang, A. Kumar, H.X. Zhang, P. Feng, R.S. Katiyar, Z.B. Wang, *J. Phys. D Appl. Phys.* **42**, 045415 (2009)
24. J. Jiang, L.P. Zhu, Y. Li, Y.M. Guo, W.S. Zhou, L. Cao, H.P. He, Z.Z. Ye, *J. Alloys Compd.* **547**, 59 (2013)

25. A. Mekki, D. Holland, C.F. McConville, M. Salim, J. Non-Cryst. Solids **208**, 267 (1996)
26. C.D. Wagner, W.M. Riggs, L.E. Davis, J.F. Moulder, G.E. Muilenberg, *Handbook of X-Ray Photoelectron Spectroscopy* (Perkin-Elmer Corporation, Physical Electronics Division, Eden Prairie, 1979), p. 55344
27. B.D. Ahn, H.S. Kang, J.H. Kim, G.H. Kim, H.W. Chang, S.Y. Lee, J. Appl. Phys. **100**, 093701 (2006)
28. A. Dadgar, A. Krtschil, F. Bertram, S. Giemisch, T. Hempel, P. Veit, A. Diez, N. Oleynik, R. Clos, J. Christen, A. Krost, Superlattices Microstruct. **38**, 245 (2005)
29. A. Krtschil, A. Dadgar, N. Oleynik, J. Blasing, A. Diez, A. Krost, Appl. Phys. Lett. **87**, 262105 (2005)
30. A. Krtschil, A. Dadgar, A. Diez, A. Krost, J. Mater. Res. **22**, 1775 (2007)
31. J. Tauc, R. Grigorovici, A. Vancu, Phys. Status Solidi **15**, 627 (1966)
32. J.H. Hong, Y.F. Wang, G. He, J.X. Wang, J. Alloys Compd. **506**, 1 (2010)
33. A.D. Acharya, S. Moghe, R. Panda, S.B. Shrivastava, M. Gangrade, T. Shripathi, D.M. Phase, V. Ganesan, Thin Solid Films **525**, 49 (2012)
34. J.J. Hopfield, D.G. Thomas, Phys. Rev. **122**, 35 (1961)
35. K. Huang, Z. Tang, L. Zhang, J. Yu, J. Lv, X. Liu, F. Liu, Appl. Surf. Sci. **258**, 3710 (2012)
36. A.F. Kohan, G. Ceder, D. Morgan, C.G.V.D. Walle, Phys. Rev. B **61**, 15019 (2000)
37. S.H. Jeong, B.S. Kim, B.T. Lee, Appl. Phys. Lett. **82**, 2625 (2003)
38. Y.J. Zeng, Z.Z. Ye, W.Z. Xu, J.G. Lu, H.P. He, L.P. Zhu, B.H. Zhao, Y. Che, S.B. Zhang, Appl. Phys. Lett. **88**, 262103 (2006)
39. W.J. Lee, J. Kang, K.J. Chang, Phys. Rev. B **73**, 024117 (2006)